AIChE

Modeling Infinite Dilution and Fickian Diffusion Coefficients of Carbon Dioxide in Water

J. Wambui Mutoru, Alana Leahy-Dios, and Abbas Firoozabadi
Dept. of Chemical Engineering, School of Engineering & Applied Science, Mason Lab, Yale University, New Haven, CT 06520

DOI 10.1002/aic.12361
Published online August 13, 2010 in Wiley Online Library (wileyonlinelibrary.com).

We propose a new model for calculating infinite dilution diffusion coefficients for carbon dioxide and water mixtures. The model takes into account temperature dependence of the dipole moment of water and polarizability of CO_2, and fits experimental CO_2—H_2O data at low and high pressures with an accuracy of 4.9%. Remarkably, the proposed model also accurately predicts infinite dilution diffusion coefficients for other binary water mixtures where solute polarizability is close to that of CO_2, such as CH_4, C_2H_6, C_3H_8, and H_2S. Moreover, we present—to the best of our knowledge—the first predictions of composition-based Fickian diffusion coefficients for CO_2—H_2O mixtures over the temperature range 298.15–413.15 K, and pressures up to 50 MPa. *AIChE J,* 57: 1617–1627, 2011
Keywords: diffusion coefficients, carbon dioxide, classical thermodynamics

Introduction

The increase in atmospheric concentrations of CO_2 is believed to be a key player in global warming, necessitating identification of viable technological options for its capture and storage. Perhaps, the most promising of these options is geoengineering which aims at the capture, transport, and injection of CO_2 into geologic strata and oceanic ecosystems with large sink capacities.[1,2] Injection of CO_2 into deep geological formations is not a new technique; it has been used in enhanced oil recovery (EOR), and recovery of coal-bed methane from unmineable coal seams.[3] For CO_2 sequestration and EOR, reservoir simulations are used to provide detailed insights on the process—its dimensions and complexities—and to help predict the long-term fate of the injected CO_2. In fact, numerical modeling studies[4,5] in porous media have shown that competing diffusion mechanisms, often neglected in such simulations, affect the flow path of injected species such as CO_2.

Quantitative description of diffusion mechanisms requires diffusion coefficients, including infinite dilution (denoted as D^{∞}) and Fickian (denoted as D) diffusion coefficients. However, experimental diffusion coefficients data available in literature for CO_2—H_2O mixtures are all at infinite dilution and limited to low temperatures and pressures. There are a few data points[6] at extremely high pressures and temperatures for applications in studies of metamorphic systems. In particular, temperatures and pressures of oil and saline formations can be up to 420 K and 50 MPa or higher; conditions at which there are no experimental diffusion data available. Hence, there is need for both infinite dilution and Fickian diffusion coefficients models that include these temperature and pressure conditions. A general formalism for Fickian diffusion coefficients is already well-established.[7]

Currently, there are no accurate models for predicting diffusion coefficients of CO_2 in water. This can be attributed to two limiting factors: one, the lack of an appropriate equation of state (EOS); and two, the absence of an accurate model for predicting infinite dilution diffusion coefficients for such mixtures that is unified at both infinite dilution extremes. The former limitation was recently resolved with the development of an accurate cubic-plus-association EOS (CPA-EOS) that explicitly accounts for association of water molecules and their cross-association with CO_2 molecules;[8] while the latter is the subject of this work.

Additional Supporting Information may be found in the online version of this article.

Correspondence concerning this article should be addressed to A. Firoozabadi at abbas.firoozabadi@yale.edu.

In this work, we develop a simple semi-empirical model that accurately describes D^{∞} for CO_2 in water at both infinite dilution limits. Furthermore, we provide to the best of our knowledge the first estimates of composition-based Fickian diffusion coefficients in CO_2-rich and water-rich mixtures. This article is organized as follows: experimental D^{∞} data in literature is outlined, followed by a brief overview of literature models and their performance in estimating D^{∞} for CO_2—H_2O mixtures. Next, details of the proposed D^{∞} model are given, followed by results and discussion of the proposed D^{∞} model and predictions for D. Finally, concluding remarks on the key findings are provided.

Experimental D^{∞} data

We conducted a survey of literature diffusion coefficients of CO_2—H_2O mixtures and found 187 data points.[9–44] Table 1 presents a summary of all CO_2—H_2O experimental data found in literature. All the data found are at infinite dilution. Note that for mixtures where composition is specified, the solute concentration is less than 5% by mole which is possibly in the infinite dilution limit. Of these, 157 experimental data points are for CO_2 infinitely diluted in water: 150 of which are from 273 to 368 K at 0.1 MPa, with the exception of two data points at high pressures of 29.4 and 39.2 MPa at 286 K (Supporting Information Table 1). There are 30 data points for water infinitely diluted in CO_2: six are at 0.1 MPa over a temperature range of 307.45–352.45 K, and 24 are in the range of 283.15–308.15 K and 13–30 MPa (Supporting Information Table 2). The remaining seven data points are for CO_2 in water at extremely high temperatures and pressures of 759.15 to 961.15 K and 1000 MPa, respectively (Supporting Information Table 3).

The interpretation of measurable quantities is simplified at the infinite dilution limit. Therefore, the reported diffusion coefficients at this limit are usually more accurate than in concentrated mixtures. Reported D^{∞} were measured using a number of experimental techniques: diaphragm cell, Stefan tube, laminar jet, wetted-wall column, wetted sphere, and horizontal film. Diffusion data at extreme temperatures and pressure found in the literature[6] were determined using an unconventional diffusion measurement technique known as a differential solubility and diffusion. Note that for this experimental technique, the errors reported in D^{∞} are large (33.3–62.5%) compared to those reported for conventional experimental techniques (3–10%).

Literature models

A number of models exist to predict the diffusion coefficients in gas and liquid mixtures as summarized by Taylor and Krishna,[7] Poling, et al.,[45] and Skelland,[46] among others. Of these models, we tested the ones relevant for CO_2—H_2O mixtures at infinite dilution (Supporting Information Table 4); most of which are semi-empirical correlations based on either the kinetic theory of Chapman-Enskog or the hydrodynamic theory of Stokes-Einstein.[47–58]

Of the tested models, two are worth mentioning here: those of Brokaw[57] and Wilke and Chang,[48] which attempt to account for association of water molecules. The former estimates D^{∞} by adding a polarity effect term to the diffusion collision integral of the Chapman-Enskog's equation that is explicitly related to the dipole moment of the polar molecule. The latter is essentially an empirical modification of the Stokes-Einstein relation; it uses an empirically-determined association factor (ϕ) for mixtures with an associating solvent such as water or alcohol. When applied to CO_2—H_2O mixtures, both Brokaw and Wilke-Chang models are hardly adequate at both infinite dilution extremes. The main limitations of these two models is that they neither account for change in the total dipole moment of water molecules with temperature, nor include the water-induced dipole moment in CO_2 molecules. The effect of polarity and induced polarity become important with temperature and pressure changes, respectively.

Table 1. Summary of Infinite Dilution Diffusion Coefficients Experimental Data for CO_2—H_2O

State	Solvent	Solute	No. of Data Points	Conditions
Gas	CO_2	H_2O	6	T: 307.45 – 352.45 K P: 0.1 MPa D^{∞}: 1.74 – 2.45 $\times 10^{-5}$ m^2/s
Liquid	CO_2	H_2O	16	T: 283.15 – 298.15 K P: 13.2 – 29.8 MPa D^{∞}: 9.6 $\times 10^{-9}$ – 2.07 $\times 10^{-8}$ m^2/s
	H_2O	CO_2	150	T: 273 – 368 K P: 0.1 – 39.2 MPa D^{∞}: 8.91 $\times 10^{-10}$ – 8.2 $\times 10^{-9}$ m^2/s
Supercritical	CO_2	H_2O	8	T: 308.15 K P: 13.47 – 29.8 MPa D^{∞}: 1.82 – 2.81 $\times 10^{-8}$ m^2/s
	H_2O	CO_2	7	T: 759.15 – 961.15 K P: 1000 MPa D^{∞}: 1.0 – 6.1 $\times 10^{-8}$ m^2/s

The performance of the models was tested against CO_2—H_2O data and the results are summarized in Tables 2 and 3. Note that not all models were tested at each infinite dilution extreme. The reason for this is twofold: one, the models are developed specifically for either gas or liquid mixtures; and two, input parameters for some models are undefined for CO_2 as a solvent (for example, the solvent association factor ϕ for the Wilke-Chang model). Models for liquid mixtures were also tested on mixtures in supercritical state. At low pressure, the tested models perform satisfactorily for D^{∞} of CO_2 in water (Figure 1a), but deviate considerably from experimental data at high pressure (Figure 1b). Similarly, for D^{∞} of water in CO_2, the models perform well at 0.1 MPa (Figure 2), but most of these models fail to capture D^{∞} at high pressure (Figure 3).

It may appear that for CO_2 infinitely diluted in water at low to high pressures, literature models would be sufficient (Table 2); however, even the best of these models—Scheibel[49]—is highly inaccurate at 1000 MPa (Table 3). For water infinitely diluted in CO_2, only the Riazi and Whiston[58] model is applicable at both low and high pressures (Table 2); but, its errors (21.9 and 31.7% at low and high pressures, respectively) are large for the high accuracy desired for infinite dilution calculations. Although the Tyn and Calus[51] (AAD = 15.4%) and Nakanishi[52] (AAD = 16.3%) models

Table 2. Summary of the Performance of Models in Estimating D^∞ for CO_2—H_2O Data Used in the Development of the Proposed D^∞ Model

Model	AAD (%)*
CO_2 in water at low pressure ($P = 0.1$ MPa, $273 \leq T \leq 368$ K)	
Othmer-Thakar (1953)[47]	7.9
Wilke-Chang (1955)[48]	8.1
Scheibel (1954)[49]	5.1
Hayduk-Laudie (1974)[50]	8.7
Tyn-Calus (1975)[51]	7.8
Nakanishi (1978)[52]	11.8
Hayduk-Minhas (1982)[53]	13.5
Siddiqi-Lucas (1986)[54]	28.1
Proposed model	4.9
CO_2 in water at high pressure ($P = 29.4$, 39.2 MPa, $T = 286$ K)	
Othmer-Thakar (1953)[47]	5.1
Wilke-Chang (1955)[48]	4.9
Scheibel (1954)[49]	5.2
Hayduk-Laudie (1974)[50]	4.9
Tyn-Calus (1975)[51]	10.3
Nakanishi (1978)[52]	15.3
Hayduk-Minhas (1982)[53]	7.3
Siddiqi-Lucas (1986)[54]	25.7
Proposed model	5.6
Water in CO_2 at low pressure ($P = 0.1$ MPa, $307.45 \leq T \leq 352.45$ K)	
Chapman-Enskog	23.5
Wilke-Lee (1955)[55]	7.3
Fuller et al (1966)[56]	22.3
Brokaw (1969)[57]	6.6
Riazi-Whitson (1993)[58]	21.9
Proposed model	6.2
Water in CO_2 at high pressure ($13.2 \leq P \leq 29.8$ MPa, $283.15 \leq T \leq 308.15$ K)	
Othmer-Thakar (1953)[47]	97.3
Scheibel (1954)[49]	153.2
Hayduk-Laudie (1974)[50]	111.7
Tyn-Calus (1975)[51]	15.4
Nakanishi (1978)[52]	16.3
Siddiqi-Lucas (1986)[54]	21.9
Riazi-Whitson (1993)[58]	31.7
Proposed model	4.5

*Absolute average deviation from N data points, $\text{AAD}(\%) = \frac{1}{N}\sum_1^N \left[\left|\frac{(D^\infty_{\text{model}} - D^\infty_{\text{exp}})}{D^\infty_{\text{exp}}}\right|\right] \times 100$.

may be sufficient for water infinitely diluted in CO_2 at high pressure, they are not strictly applicable in the gas phase; when tested at low pressure for water in CO_2, they each have an AAD > 99%. Therefore, we emphasize that to the best of our knowledge, there is currently no single model that is applicable in estimating D^∞ for CO_2—H_2O mixtures at low and high pressures for both infinite dilution extremes. Unlike these models, our proposed model is accurate for CO_2—H_2O at both D^∞ limits and is applicable at low and high pressures. High accuracy of D^∞ is desirable since the calculation of D involves D^∞ (see Appendix).

Proposed D^∞ model

We believe that a D^∞ model for CO_2—H_2O mixtures that is accurate at both infinite dilution limits should adequately account for the polar nature of water molecules and the polarizability of CO_2 molecules. As our results show, these contributions become important with changing temperatures and pressures, respectively. Intrinsically, water molecules have a large permanent dipole moment that causes formation of aggregates of its molecules. On the contrary, CO_2 has no net dipole moment, but due to its polarizability, it can have one induced in the presence of an electric field.[59] When a water molecule approaches a CO_2 molecule, a dipole-induced-dipole interaction is produced—resulting in the formation of water-CO_2 clusters—that affects the solvation of CO_2 in water.[60,61] Molecular dynamic studies have confirmed distinct hydrogen bonding between the oxygen of CO_2 and the hydrogen of water.[62]

The unified D^∞ model proposed here—that is semi-empirical and based in part on corresponding-state theory—takes into account the temperature effect on the total dipole moment of water and the induced-dipole moment on CO_2, along with other thermodynamic variables. A single expression describing D^∞ of water infinitely diluted in CO_2 as well as CO_2 infinitely diluted in water as a function of temperature, pressure, molecular mass, dipole moment, molar density and viscosity was found to be,

$$D_{12}^\infty = \frac{k_1 (M_{12}\mu_{12})^{k_2} T_{r,2}^{k_3}}{P_{r,2}^{k_4} (\eta_2 c_2)^{k_5}}, \quad (1)$$

where,

$$M_{12} = \left(\frac{1}{M_{H_2O}} + \frac{1}{M_{CO_2}}\right)^{-1}, \quad (2)$$

$$\mu_{12} = \frac{\mu_2}{\mu_1}, \quad (3)$$

$$\begin{aligned} k_1 &= 10^{-7.23389}, \\ k_2 &= 1.35607 \times 10^{-1}, \\ k_3 &= 1.84220 \times 10^{0}, \\ k_4 &= 2.41943 \times 10^{-3}, \\ k_5 &= 8.58204 \times 10^{-1}. \end{aligned} \quad (4)$$

In Eqs. 1–3, subscripts 1 and 2 refer to the component at infinite dilution (solute), and of the dominant component (solvent) in the mixture, respectively; M is the molecular mass in g/mol; μ is the total dipole moment in C.m; $T_{r,2}$ and $P_{r,2}$ are reduced temperature and pressure of the solvent, respectively; η_2 is solvent viscosity in Pa s, and c_2 is solvent molar density in mol/m^3. Equation 4 shows the five constants used in Eq. 1. These parameters were obtained via nonlinear least squares minimization of the 180 data points provided in Supporting Information Tables 1 and 2 for

Table 3. Summary of the Performance of Models in Estimating D^∞ for CO_2—H_2O Mixtures not Used in the Development of Proposed D^∞ Model ($759.15 \leq T \leq 961.15$ K, $P = 1000$ MPa)

Model	AAD (%)
Othmer-Thakar (1953)[47]	44.7
Wilke-Chang (1955)[48]	164.4
Scheibel (1954)[49]	178.7
Hayduk-Laudie (1974)[50]	52.1
Tyn-Calus (1975)[51]	197.3
Nakanishi (1978)[52]	210.7
Hayduk-Minhas (1982)[53]	205.2
Siddiqi-Lucas (1986)[54]	120.4
Proposed model	84.9

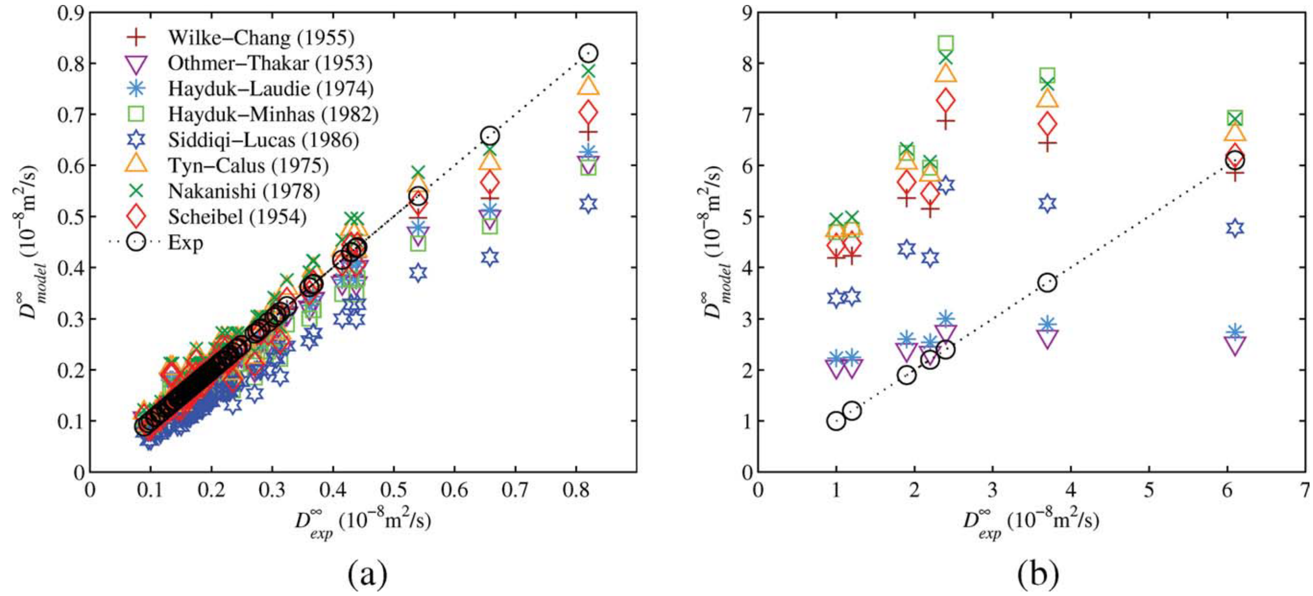

Figure 1. (a,b) Diffusion coefficients of CO_2 infinitely diluted in water (D^{∞}) at (a) 0.1 MPa and (b) high pressure: experimental data (circles, dashed line) and literature models (various shapes).

The performance of the models is between 8.1 and 28.1% AAD for 148 experimental data points at 0.1 MPa ($273 \leq T \leq 368$ K), and between 35.9 and 167.3% AAD for the two data points at 29.4 and 39.2 MPa ($T = 286$ K) and the seven data points at 1000 MPa ($759.15 \leq T \leq 961.15$ K). [Color figure can be viewed in the online issue, which is available at wileyonlinelibrary.com.]

CO_2—H_2O mixtures in the gas, liquid, and supercritical states over the temperature range 273–368 K and pressure range 0.1–39.2 MPa. Note that the seven data points at 1000 MPa were not used in generating the model constants due to their high experimental errors.

Analysis of the constants in Eq. 4 makes it apparent that for CO_2—H_2O mixtures, D^{∞} is a stronger function of temperature than of pressure. However, the small pressure contribution cannot be neglected because the experimental data considered is limited mainly to atmospheric pressure with only a few data points at higher pressures (13.2–39.2 MPa). Intuitively, at higher pressure this contribution becomes more pronounced; high pressure influences equilibrium compositions, and the extent of intermolecular interactions and, therefore, substantially affects D as seen in the results

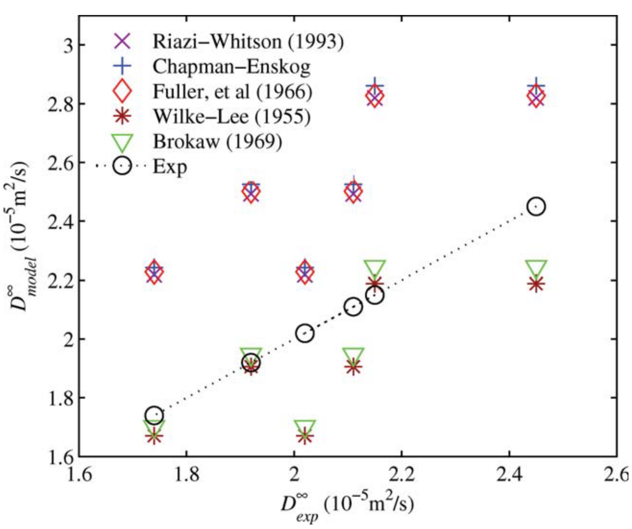

Figure 2. Diffusion coefficients of water infinitely diluted in CO_2 (D^{∞}) at a low pressure of 0.1 MPa: experimental data (circles, dashed line) and literature models (various shapes).

The performance of the models is between 6.6 and 23.5% AAD for 6 data points ($307.45 \leq T \leq 352.45$ K). [Color figure can be viewed in the online issue, which is available at wileyonlinelibrary.com.]

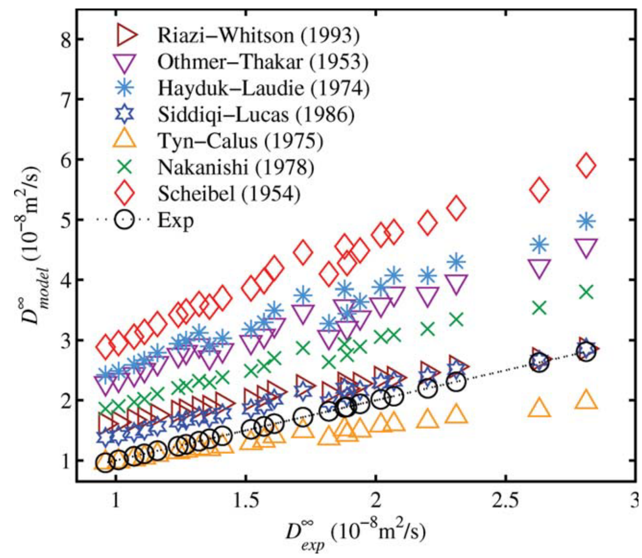

Figure 3. Diffusion coefficients of water infinitely diluted in CO_2 (D^{∞}) at high pressure ($13.2 \leq P \leq 29.8$ MPa): experimental data (circles, dashed line) and literature models (various shapes).

The performance of the models is between 15.4 and 153.2% AAD for 24 data points ($283.15 \leq T \leq 308.15$ K). [Color figure can be viewed in the online issue, which is available at wileyonlinelibrary.com.]

section. Moreover, both η_2 and c_2 are strong functions of temperature and weak functions of pressure; their small pressure dependence is important when dealing with high pressures of saline aquifers and oil/natural gas reservoirs.

In Eq. 1, the solvent molar density and viscosity are determined from specific correlations based on experimental data.[63] The total molecular dipole moment for water in liquid phase (μ_{H_2O}) is calculated as a function of temperature based on Gubskaya and Kusalik.[64,65] The formulation itself is mathematically involved, but can be succinctly reproduced in the form of an interpolation equation:

$$\mu_{H_2O} = -1.2142 \times 10^{-32}T + 2.1236\mu_o, \quad (5)$$

where, T is the temperature in K and μ_o is the dipole moment in C.m of water molecules in vapor phase.

The water-induced total dipole moment in CO_2 is determined from the electric field (E_{field}) generated by water molecules and the polarizability (α) of CO_2 molecules[59]:

$$\mu_{CO_2} = \alpha_{CO_2} E_{field}, \quad (6)$$

Molecular polarizability used in Eq. 6 is obtained from the CRC Handbook of Chemistry and Physics,[66] and the E_{field} is calculated from the dipole moment of water as a function of temperature (μ_{H_2O}), the dielectric constant of water (ε_{H_2O}), and the separation between CO_2 and water molecules (r):

$$E_{field} = \frac{\mu_{H_2O}}{2\pi\varepsilon_{H_2O} r^3}, \quad (7)$$

The dielectric constant of water (ε_{H_2O}) in Eq. 7 is estimated as function of temperature from the interpolation equation given by Uematsu and Frank[67]:

$$\varepsilon_{H_2O} = 1 + \left(\frac{a_1}{T^*}\right)\rho^* + \left(\frac{a_2}{T^*} + a_3 + a_4 T^*\right)\rho^{*^2} + \left(\frac{a_5}{T^*} + a_6 T^* + a_7 T^{*^2}\right)\rho^{*^3} + \left(\frac{a_8}{T^{*^2}} + \frac{a_9}{T^*} + a_{10}\right)\rho^{*^4}, \quad (8)$$

where,

$$T^* = \frac{1}{298.15}T, \quad (9)$$

$$\rho^* = c_{H_2O} M_{H_2O} \times 10^{-6}, \quad (10)$$

$$\begin{aligned} a_1 &= 7.62571 \times 10^0, \\ a_2 &= 2.44003 \times 10^2, \\ a_3 &= -1.40569 \times 10^2, \\ a_4 &= 2.77841 \times 10^1, \\ a_5 &= -9.62805 \times 10^1, \\ a_6 &= 4.17909 \times 10^1, \\ a_7 &= -1.02099 \times 10^1, \\ a_8 &= -4.52059 \times 10^1, \\ a_9 &= 8.46395 \times 10^1, \\ a_{10} &= -3.58644 \times 10^1. \end{aligned} \quad (11)$$

The challenge to using Eq. 7 is determining the separation, r. We assume that r can be estimated as half the collision diameter given by an intermolecular force law as suggested by Cussler[68]:

$$r \approx \frac{1}{2}\sigma_{12}, \quad (12)$$

In our work, we account for both the dipole moment of water and polarizability of CO_2 as functions of temperature. Therefore, we chose to work with the tabulated pure component Lenard-Jones and Stockmayer potentials[69] for the length (σ) and energy (ζ) parameters for CO_2 and water, respectively. We use the combination law by Hirschfelder, et al.[69] to calculate σ_{12}:

$$\sigma_{12} \approx \frac{1}{2}(\sigma_{CO_2} + \sigma_{H_2O})\xi^{-1/6}, \quad (13)$$

where, ξ is calculated from the polarizability of the nonpolar molecule (α), dipole moment (μ) of the polar molecule, and pure component ζ:

$$\xi = \left[1 + \frac{1}{4}\alpha^*_{CO_2}\mu^{*2}_{H_2O}\sqrt{\frac{\zeta_{H_2O}}{\zeta_{CO_2}}}\right], \quad (14)$$

where,

$$\alpha^*_{CO_2} = \frac{\alpha_{CO_2}}{\sigma^3_{CO_2}}, \quad (15)$$

$$\mu^*_{H_2O} = \frac{\mu_{H_2O}}{\sqrt{\zeta_{H_2O}\sigma^3_{H_2O}}}. \quad (16)$$

Results and Discussion

Performance of the proposed D^∞ model

The proposed D^∞ model (Eq. 1) fits well to the 180 experimental data points for CO_2—H_2O mixtures used in its development as shown in Figure 4. The model accurately captures the experimental data with an accuracy of 4.9% AAD.* Note that the model covers four orders of magnitude of D^∞ from 10^{-9} to 10^{-5} m^2/s. Performance of the proposed D^∞ model is compared to experimentally reported data for four classes of binary water mixtures not used in the model development with the solutes: CO_2 at 1000 MPa; nonpolar, but polarizable alkane molecules, methane (CH_4) and ethane (C_2H_6); slightly polar linear alkane molecules, propane (C_3H_8), n-butane (nC_4H_{10}), and n-pentane (nC_5H_{12}); and fairly polar hydrogen sulfide (H_2S). The results of our proposed D^∞ model on these binary mixtures are shown in Figures 5–8.

Figure 5 compares the proposed D^∞ model to CO_2—H_2O experimental data[6] not used in its development (last row of Table 1) taking into account the extreme pressure. For this data set, concentration of CO_2 was determined to be 3% (by mole) or less; a composition indicative of infinite dilution. As shown in Figure 5, the predictions of our proposed model are acceptable. Moreover, the model makes the linearity in D^∞ apparent; a trend that is obscured by the large scatter in experimental data. As noted earlier, reported errors in

*Absolute average deviation from N data points, $\text{AAD}(\%) = \frac{1}{N}\sum_1^N \left[\left|\frac{(D^\infty_{model} - D^\infty_{exp})}{D^\infty_{exp}}\right|\right] \times 100.$

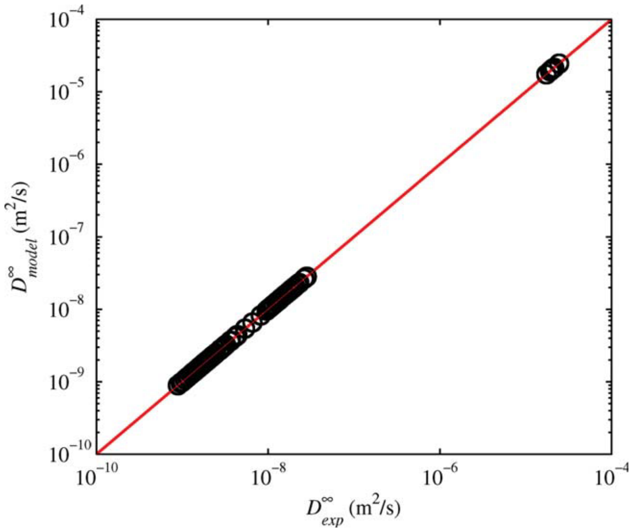

Figure 4. Diffusion coefficients of CO_2 and water at infinite dilution (D^{∞}): 180 experimental data (circles) and the model given in Eq. 1 (solid line) for $273 \leq T \leq 368$ K, $0.1 \leq P \leq 39.2$ MPa, and $8.91 \times 10^{-10} \leq D^{\infty} \leq 2.45 \times 10^{-5}$ m^2/s.

The AAD of the proposed D^{∞} model is 4.9%. [Color figure can be viewed in the online issue, which is available at wileyonlinelibrary.com.]

experimental data are high; hence, 84.9% AAD in our D^{∞} model predictions is not necessarily a reflection of its inadequacy. Although it appears that the Othmer and Thakar[47] and Hayduk and Laudie[50] models perform better than the proposed model for this data set (Table 3), these models have higher AAD than the proposed D^{∞} model at low and high pressures, especially for water infinitely diluted in CO_2 (Table 2).

Table 4. Summary of Experimental Data for Infinite Dilution of Alkanes and H_2S in Liquid Water Used to Test the Proposed D^{∞} Model

Solute	No. of Data Points	Conditions
CH_4	17	T: 274.9 − 342.8 K D^{∞}: $8.13 \times 10^{-10} - 4.48 \times 10^{-9}$ m^2/s
C_2H_6	8	T: 277.15 − 333.15 K D^{∞}: $6.9 \times 10^{-10} - 2.94 \times 10^{-9}$ m^2/s
C_3H_8	8	T: 277.15 − 333.15 K D^{∞}: $5.5 \times 10^{-10} - 2.71 \times 10^{-9}$ m^2/s
nC_4H_{10}	8	T: 277.15 − 333.15 K D^{∞}: $5.0 \times 10^{-10} - 2.51 \times 10^{-9}$ m^2/s
nC_5H_{12}	4	T: 277.15 – 333.15 K D^{∞}: $4.6 \times 10^{-10} - 2.24 \times 10^{-9}$ m^2/s
H_2S	11	T: 288.15 – 368 K D^{∞}: $1.53 - 5.49 \times 10^{-9}$ m^2/s

All Data are at 0.1 MPa.

Table 4 summarizes the mixture conditions and range of D^{∞} data for alkane—water and H_2S—H_2O mixtures.[24,70–75] The data points are provided in Supporting Information Table 5. We chose to use linear alkane molecules and H_2S due to their similarity to CO_2 in polarizability[66] and low-pressure solubility,[76] the availability of their respective D^{∞} over a range of temperature, and their applicability in natural gas and oil reservoir systems. In testing the proposed D^{∞} model, the polarizability (α) and collision diameter (σ) of CO_2 in Eqs. 6, and 13–15, were replaced with those of the alkane or H_2S.

Figure 6 compares experimental data to the proposed D^{∞} model for CH_4—H_2O and C_2H_6—H_2O mixtures as a function of temperature at 0.1 MPa. As shown, our proposed D^{∞} model accurately reproduces the reported experimental values. Both CH_4 and C_2H_6—like CO_2—have zero dipole moment, but have polarizabilities ($\alpha_{CH_4} = 2.60 \times 10^{-30}$m^3, $\alpha_{C_2H_6} = 4.45 \times 10^{-30}$m^3) close in value to the polarizability

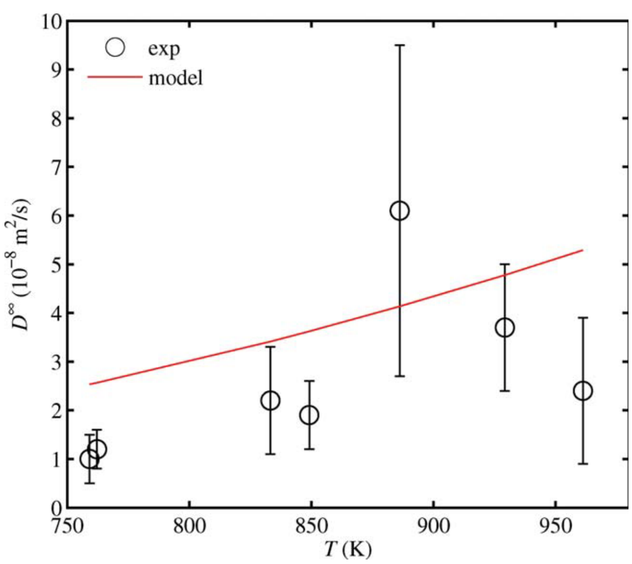

Figure 5. Infinite dilution diffusion coefficients (D^{∞}) vs. temperature (T) for CO_2-H_2O at 1000 MPa.

The AAD of the proposed D^{∞} model is 84.9%, and the reported error in experimental data (7 data points) varies from 33.3 to 62.5%. [Color figure can be viewed in the online issue, which is available at wileyonlinelibrary.com.]

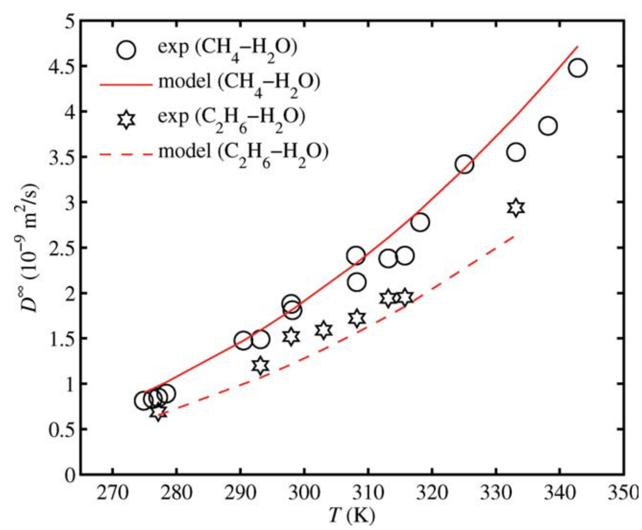

Figure 6. Infinite dilution diffusion coefficients (D^{∞}) vs. temperature (T) for CH_4—H_2O and C_2H_6—H_2O mixtures at 0.1 MPa.

The AAD of the proposed D^{∞} model is 8.1% for CH_4—H_2O (17 data points) and 10.6% for C_2H_6—H_2O (eight data points). [Color figure can be viewed in the online issue, which is available at wileyonlinelibrary.com.]

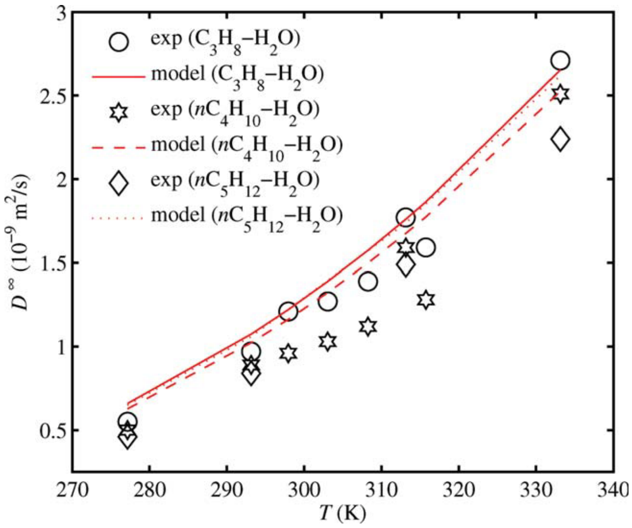

Figure 7. Infinite dilution diffusion coefficients (D^∞) vs. temperature (T) for C_3H_8—H_2O, nC_4H_{10}—H_2O, and nC_5H_{12}—H_2O mixtures at 0.1 MPa.

The AAD of the proposed D^∞ model is 9.2% for C_3H_8—H_2O (eight data points), 21% for nC_4H_{10}—H_2O (eight data points), and 25.3% for nC_5H_{12}—H_2O (four data points). [Color figure can be viewed in the online issue, which is available at wileyonlinelibrary.com.]

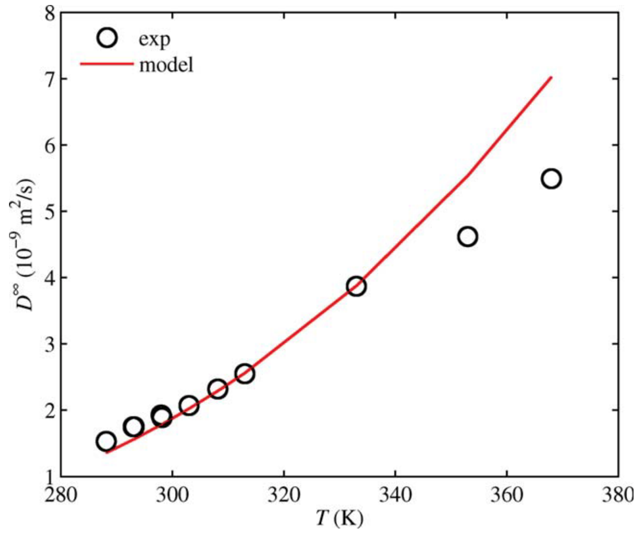

Figure 8. Infinite dilution diffusion coefficients (D^∞) vs. temperature (T) for H_2S—H_2O mixtures at 0.1 MPa.

The AAD of the proposed D^∞ model is 8.9% for 11 data points. [Color figure can be viewed in the online issue, which is available at wileyonlinelibrary.com.]

of CO_2 ($\alpha_{CO_2} = 2.91 \times 10^{-30} m^3$); thus, the proposed model performs equally well for CH_4—H_2O and C_2H_6—H_2O mixtures. Figure 7 shows the plot of D^∞ over the temperature range of 277.15–333.15 K for C_3H_8—H_2O, nC_4H_{10}—H_2O, and nC_5H_{12}—H_2O mixtures at 0.1 MPa. As shown, the model reproduces experimental values for C_3H_8—H_2O quite well, but has higher deviations for nC_4H_{10}—H_2O and nC_5H_{12}—H_2O. It is worth noting the large disparity in reported D^∞ between the two data sets for nC_4H_{10}—H_2O at temperatures from 310 to 320 K.[73,74]

There is a trend in the performance of the model based on the polarizability of the alkane (Table 5): for small alkane molecules (CH_4, C_2H_6, and C_3H_8) whose polarizability is close to that of CO_2—regardless of their net dipole moment—the model predictions are fairly accurate (AAD ~ 10%) for a comparable temperature range. However, for the longer linear alkanes (nC_4H_{10} and nC_5H_{12}), whose polarizability is almost three times or more that of CO_2, performance of the model deteriorates (AAD > 20%). Fortunately, smaller alkane molecules have a higher probability of being present as impurities in CO_2 injection streams than larger alkane molecules. Our proposed D^∞ model can describe accurately their diffusion in water if their amounts are non-negligible and need to be accounted for.

Table 5. Summary of the Performance of Proposed D^∞ Model for Infinite Dilution of Alkane and H_2S in Water

Mixture	Polarizability (10^{-30} m^3)	Dipole Moment at STP (Debye)	AAD (%)
CH_4—H_2O	2.6	0	8.1
C_2H_6—H_2O	4.45	0	10.6
C_3H_8—H_2O	6.29	0.084	9.2
nC_4H_{10}—H_2O	8.2	0.05	21.0
nC_5H_{12}—H_2O	9.99	0.37	25.3
H_2S—H_2O	3.8	0.97	8.9

Figure 8 shows experimental and predicted D^∞ for H_2S—H_2O mixtures at 0.1 MPa over the temperature range of 288.15–368.15 K. Remarkably, the proposed D^∞ model works well for H_2S—H_2O mixtures. It is interesting to note that the model has higher accuracy for the more polar H_2S (AAD = 8.9%) than it does for the less polar nC_4H_{10} and nC_5H_{12} (Table 5). This can be explained in terms of the differences in polarizability; molecular polarizability of H_2S ($\alpha_{H_2S} = 3.80 \times 10^{-30} m^3$) is close to that of CO_2 ($\alpha_{CO_2} = 2.91 \times 10^{-30} m^3$) unlike nC_4H_{10} ($\alpha_{nC_4H_{10}} = 8.2 \times 10^{-30} m^3$) and nC_5H_{12} ($\alpha_{nC_5H_{12}} = 9.99 \times 10^{-30} m^3$) whose polarizabilities are higher than that of CO_2. Clearly, accounting for dipole-induced-dipole interactions between water and polarizable molecules is important for D^∞ calculations.

Predictions of the effect of composition on D

All the available CO_2—H_2O data are given at the infinite dilution limits; therefore, we assess the effect of increasing composition on diffusion coefficients. To this end, we have employed the general formalism (see Appendix) frequently used for calculating Fickian diffusion coefficients (D) from D^∞.[7] The formalism itself is sequential: starting from D^∞, the composition-dependent Maxwell-Stefan diffusion coefficients ($\wp$) are calculated. Subsequently, the mixture's nonideality (Γ) is accounted for to determine D. Indeed, this approach was successfully used recently to model diffusion coefficients of hydrocarbon mixtures.[77]

The composition of CO_2 in water at saturation is a function of temperature and an even stronger function of pressure; CO_2 solubility in water decreases slightly with increases in temperature, but increases markedly with increases in pressure.[78,79] Hence, for given initial mixture

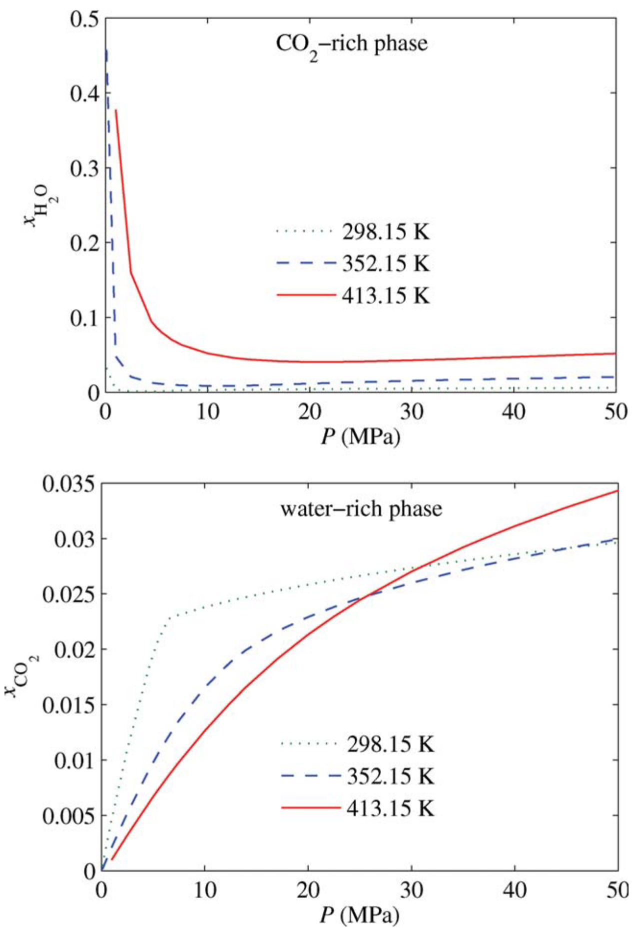

Figure 9. Calculated compositions of water (x_{H_2O}) and CO_2 (x_{CO_2}) vs. pressure (*P*) in the CO_2-rich and water-rich phases, respectively, at 298.15, 352.15, and 413.15 K.

[Color figure can be viewed in the online issue, which is available at wileyonlinelibrary.com.]

conditions (composition of CO_2 and water, temperature, and pressure), we use the CPA-EOS to perform a two-phase flash calculation that provides—by density difference—the equilibrium compositions of the CO_2-rich and water-rich phases. Subsequently, we assess the composition-dependence of *D*—using the established Fickian diffusion model—over a pressure and temperature range of 50 MPa, and 298.15 to 413.15 K, respectively. Figure 9 shows the phase compositions over this temperature and pressure range.

The CPA-EOS used in this work was initially tested to a maximum pressure of 18.17 MPa at a temperature of 533.15 K for phase compositions of CO_2—H_2O mixtures;[8] a pressure too low for the purposes of this work. Therefore, it was necessary to test the CPA-EOS at higher pressures to ensure its validity at high temperature (~420 K) and pressure (≥50 MPa) conditions of interest in this work. To this end, performance of the CPA-EOS was tested against phase equilibria data available in literature[80,81] for CO_2—H_2O mixtures. As shown in Table 6, the predicted composition of CO_2 from the CPA-EOS agrees well with experimental data. Conclusively, the CPA-EOS phase-equilibria calculations are

Table 6. Predicted Composition of CO_2 (in CO_2—H_2O Mixtures) from the CPA-EOS Compared to Experimental Values at Given Temperatures and Pressures

P (MPa)	*T* (K)	Calc. Composition (x_{CO_2})	Exp. Composition (x_{CO_2})	Dev. (%)[a]
169.2	500.95	0.765	0.789[b]	3.1
264.5	534.95	0.625	0.625[b]	0
280.0	538.15	0.608	0.578[c]	5.2
300.0	538.15	0.607	0.670[c]	9.4
311.1	546.45	0.562	0.530[b]	6.1

[a]Percent deviation, Dev (%) $= \left(\frac{x_{CO_2,exp} - x_{CO_2,CPA-EOS}}{x_{CO_2,exp}}\right) \times 100$.
[b]Ref. 80.
[c]Ref. 81.

sufficiently accurate at high temperature and pressure. It is worth noting the availability of a recently published cubic EOS based on the Gibbs-Helmholtz equation.[82] This EOS was tested against experimental densities of CO_2 and CO_2-water mixtures, as well as specific volumes of water, at low temperatures and high pressures; however, it was not tested for phase composition predictions like the CPA-EOS used in this work.

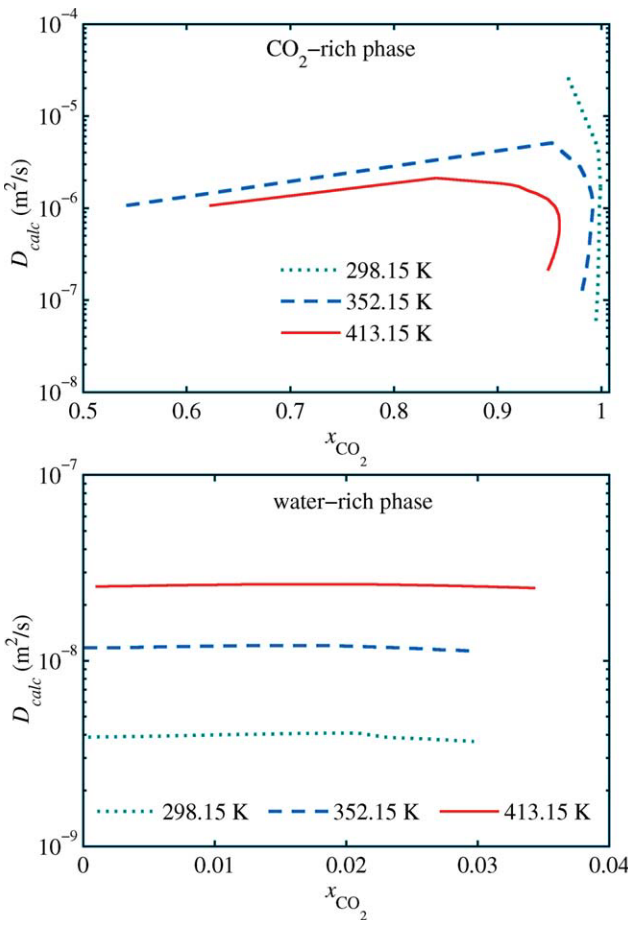

Figure 10. Calculated Fickian diffusion coefficients (D_{calc}) vs. the equilibrium concentration of CO_2 (x_{CO_2}) in the CO_2-rich and water-rich phases at 298.15, 352.15, and 413.15 K.

[Color figure can be viewed in the online issue, which is available at wileyonlinelibrary.com.]

Figure 10 shows the computed results of D as a function of concentration of CO_2 (x_{CO_2}) at 298.15, 352.15, and 413.15 K in the CO_2-rich and water-rich phases. As expected, D is a strong function of temperature in the CO_2-rich and water-rich phases; in the water-rich phase, there is an order of magnitude increase in D with temperature increase from 298.15 to 413.15 K. At high temperature, the extent of association of water molecules is lower, which contributes to the higher D. Composition-dependence of D is strong in the CO_2-rich phase, particularly at high x_{CO_2} where D decreases rapidly. The pressure range in Figure 10 is from 0.1 to 50 MPa. Hence, the effect of composition on D is mutually coupled with that of pressure, since for CO_2—H_2O mixtures, increased CO_2 concentration cannot be achieved without increasing pressure (Figure 9). Note that at high pressure, there is a higher degree of intermolecular cross-association between CO_2 and water molecules, which plays a role in the lower D.

Concluding Remarks

In this work, a simple model is proposed for calculating infinite dilution diffusion coefficients, D^∞, of CO_2—H_2O mixtures. The proposed model takes into account the intrinsic dipole moment of water molecules as a function of temperature, and the polarizability of CO_2 molecules (which induces a dipole moment on the CO_2 molecule in the presence of an electric field created by surrounding water molecules). The proposed model is applicable at both infinite dilution extremes—unlike all other models in literature—and fits well to CO_2—H_2O experimental data at low and high temperatures and pressures with an accuracy of 4.9% on average.

Comparing the proposed D^∞ model to CO_2—H_2O experimental data at 759.15 to 961.15 K and 1000 MPa gives results comparable in accuracy of reported experimental data. The performance of our D^∞ model highlights the feasibility of its extension to extreme pressures; an indication that the model would work well at high pressures typical of oil reservoirs and saline aquifers. Moreover, the proposed D^∞ model, with the adjustable parameters based on CO_2—H_2O data, performs equally well for binary mixtures of water with short alkane molecules (CH_4, C_2H_6, and C_3H_8) as well as H_2S whose polarizability and low-pressure solubility are comparable to that of CO_2. This points to the importance of dipole-induced-dipole interactions on diffusion at infinite dilution.

It should be noted that since our proposed D^∞ model accurately predicts D^∞ for CO_2—H_2O, H_2S—H_2O, and CH_4—H_2O, it could potentially be generalized to model D in ternary mixtures such as CO_2—H_2S—H_2O. In practice, CO_2 injected in saline aquifers might contain non-negligible amounts of either H_2S or CH_4 as contaminants; therefore, being able to model a third component would be useful. The only limitation to such a generalization is the lack of experimental data to verify infinite dilution diffusion coefficients for three-component mixtures.

Predictions for composition-based Fickian diffusion coefficients, D, for CO_2—H_2O mixtures reveal the competing effects of temperature and pressure on D. Whereas increase in temperature increases D in both the CO_2-rich and water-rich phases, increasing pressure noticeably decreases D in the CO_2-rich phase. This large pressure effect is mutually coupled with that of increased CO_2 composition. Moreover, the extent of intermolecular associations (which are functions of temperature, pressure, and composition) affect D. These composition-based results imply that greatly varying rates of diffusion should be expected for specific composition, temperature, and pressure conditions of a given oil reservoir or saline aquifer.

Acknowledgments

This work was financially supported by the Petroleum Research Fund Grant PRF 45927-AC9 of the American Chemical Society to Yale University, and by ConocoPhillips. The authors gratefully acknowledge the assistance of Dr. Zhidong Li of RERI with the CPA-EOS.

Notation

$a_1 - a_{10}$ = regression constants for interpolation equation for ε_{H_2O}
c = molar density (mol/m^3)
D = Fickian diffusion coefficients in binary mixtures (m^2/s)
D^∞ = diffusion coefficient at infinite dilution (m^2/s)
f_i = fugacity of component i (Pa)
$\vec{J}$ = molar diffusive flux (mol/m^{2}s)
k_i = regression constants for Eq. 1
k_B = Boltzmann's constant (m^2 kg/s^2 K)
M_i = molecular mass of component i (g/mol)
n = number of carbon atoms in linear alkane molecules
N = total number of data points
P = pressure (MPa)
r = separation between diffusing molecules (m)
T = temperature (K)
x_i = mole fraction of component i

Greek letters

α = polarizability of the nonpolar molecule (m^3)
Γ = nonideality factor
ε = dielectric constant
ζ = characteristic energy of the intermolecular force law (J)
η = viscosity (Pa.s)
μ = dipole moment (C.m)
ρ = mass density (kg/m^3)
σ = characteristic length of the intermolecular force law (m)
∇x_i = gradient of mole fraction of component i (m^{-1})
$\wp$ = Stefan-Maxwell diffusion coefficient (m^2/s)

Subscripts

calc = D calculated from the general Fickian diffusion coefficients framework
exp = D^∞ from experimental measurements found in literature
model = D^∞ calculated from the proposed model (Eq. 1)
r = reduced temperature or pressure
1 = component at infinite dilution, the solute
2 = dominant component, the solvent

Literature Cited

1. House KZ, Schrag DP, Harvey CF, Lackner KS. Permanent CO_2 storage in deep-sea sediments. *PNAS*. 2006;103:12291–12295.
2. Broecker WS. CO_2 capture and storage: possibilities and perspectives. *Elements*. 2008;4:296–297.
3. Lal R. Sequestering atmospheric carbon dioxide. *Crit Rev in Plant Sci*. 2009;28:90–96.
4. Ghorayeb K, Firoozabadi A. Modeling multicomponent diffusion and convection in porous media. *SPE J*. 2000;5:158–171.
5. Hoteit H, Firoozabadi A. Numerical modeling of diffusion in fractured media for gas-injection and -recycling schemes. *SPE J*. 2009; 14:323–337.
6. Wark DA, Watson EB. Interdiffusion of H_2O and CO_2 in metamorphic fluids at 490 to 690 °C and 1 GPa. *Geochim Cosmochim Acta*. 2004;68:2693–2698.

7. Taylor R, Krishna R. *Multicomponent Mass Transfer*. New York: Wiley, 1993.
8. Li Z, Firoozabadi A. Cubic-plus-association equation of state for water-containing mixtures: is "cross association" necessary? *AIChE J*. 2009;55:1803–1813.
9. Vivian JE, King CJ. Diffusivities of slightly soluble gases in water. *AIChE J*. 1964;10:220–221.
10. Mazarei AF, Sandall OC. Diffusion coefficients for helium, hydrogen, and carbon dioxide in water at 25°C. *AIChE J*. 1980;26:154–157.
11. Ng WY, Walkley J. Diffusion of gases in liquids: the constant size bubble method. *Can J Chem*. 1969;47:1075–1077.
12. Maharajh DM, Walkley DJ. The temperature dependence of the diffusion coefficients of Ar, CO_2, CH_4, CH_3Cl, CH_3Br, and $CHCl_2F$ in water. *Can J Chem*. 1973;51:944–952.
13. Tang YP, Himmelblau DM. Effect of solute concentration on the diffusivity of carbon dioxide in water. *Chem Eng Sci*. 1965;20:7–14.
14. Pratt KC, Slatter DH, Wakeham WA. A rapid method for the determination of diffusion coefficients of gases in liquids. *Chem Eng Sci*. 1973;28:1901–1903.
15. Tan KK, Thorpe RB. Gas diffusion into viscous and non-newtonian liquids. *Chem Eng Sci*. 1992;47:3565–3572.
16. Bodnar LH, Himmelblau DM. Continuous measurement of the diffusion coefficients of gases in liquids using glass scintillators. *Int J Appl Radiat Isot*. 1962;13:1–6.
17. Unver AA, Himmelblau DM. Diffusion coefficients of CO_2, C_2H_4, C_3H_6 and C_4H_8 in water from 6 to 65°C. *Chem Eng Data*. 1964;9:428–431.
18. Cullen EJ, Davidson JF. Absorption of gases in liquid jets. *Trans Faraday Soc*. 1956;52:113–120.
19. Reddy KA, Doraiswamy LK. Estimating liquid diffusivity. *Ind Eng Chem Fundamen*. 1967;6:77–79.
20. Scriven LE. Interfacial resistance in gas absorption. [Ph.D. Dissertation]. United States—Delaware: University of Delaware, 1956.
21. Woods DR. Mass transfer between a liquid jet and a countercurrent gas stream. Ph.D. Dissertation; United States—Wisconsin: University of Wisconsin-Madison, 1961.
22. Ferrell RT, Himmelblau DM. Diffusion coefficients of nitrogen and oxygen in water. *J Chem Eng Data*. 1967;12:111–115.
23. Duda JL, Vrentas JS. Laminar liquid jet diffusion studies. *AIChE J*. 1968;14:286–294.
24. Tamimi A, Rinker EB, Sandall OC. Diffusion coefficients for hydrogen sulfide, carbon dioxide, and nitrous oxide in water over the temperature range 293–368 K. *J Chem Eng Data*. 1994;39:330–332.
25. Thomas WJ, Adams MJ. Measurement of the diffusion coefficients of carbon dioxide and nitrous oxide in water and aqueous solutions of glycerol. *Trans Faraday Soc*. 1965;61:668–673.
26. Frank MJW, Kuipers JAM, van Swaaij WPM. Diffusion coefficients and viscosities of CO_2+H_2O, CO_2+CH_3OH, NH_3+H_2O, and NH_3+CH_3OH liquid mixtures. *J Chem Eng Data*. 1996;41:297–302.
27. Jähne B, Heinz G, Dietrich W. Measurement of the diffusion coefficients of sparingly soluble gases in water. *J Geophys Res*. 1987;92:10767–10776.
28. Leaist DG. Diffusion of aqueous carbon dioxide, sulfur dioxide, sulfuric acid, and ammonia at very low concentrations. *J Phys Chem*. 1987;91:4635–4638.
29. Tham MJ, Bhatia KK, Gubbins KE. Steady-state method for studying diffusion of gases in liquids. *Chem Eng Sci*. 1967;22:309–311.
30. Sovova H, Prochazka J. A new method of measurement of diffusivities of gases in liquids. *Chem Eng Sci*. 1976;31:1091–1097.
31. Himmelblau DM. Diffusion of dissolved gases in liquids. *Chem Rev*. 1964;64:527–550.
32. Brignole EA, Echarte R. Mass transfer in laminar liquid jets measurement of diffusion coefficients. *Chem Eng Sci*. 1981;36:695–703.
33. Peaceman DW. Liquid-side resistance in gas absorption with and without chemical reaction. Ph.D. Dissertation, United States—Massachusetts: Massachusetts Institute of Technology, 1952.
34. Ringbom A. Über die bestimmung der diffusionskoeffizienten von gasen in flüssigkeiten, *Z Anorg Allgem Chem*. 1938;238:94–102.
35. Norman WS, Sammak FYY. Gas absorption in a packed column-Part 1: The effect of liquid viscosity on the mass transfer coefficient. *Trans Inst Chem Engrs*. 1963;41:109–116.
36. Onda K, Okamoto T, Yamaji Y. Measurement of the diffusivities of CO_2 in liquids by liquid jets. *Kagaku Kogaku*. 1960;24:918–925.
37. Nijsing RATO, Hendtiksz RH, Kramers H. Absorption of CO_2 jets and falling films of electrolyte solutions, with and without chemical reaction. *Chem Eng Sci*. 1959;10:88–104.
38. Hufner G. Über die bestimmung der diffusion-coefficienten einiger gase für wasser. *Ann Phys Chem*. 1897;60:134.
39. Stefan J. Über die diffusion der kohlensaure durch wasser und alkohol. *S. B. Akad Wiss Wien Math Naturwiss Kl Abt*. 1878;77:371–409.
40. Tamman J, Jessen V. Über die diffusionskoeffizienten von gasen in wasser und ihre temperaturabhängigkeit. *Z Anorg Allegm Chem*. 1929;179:125–144.
41. Hirai S, Okazaki K, Yazawa H, Ito H, Tabe Y, Hijakata K. Measurement of CO_2 diffusion coefficient and application of LIF in pressurized water. *Energy*. 1997;22:363–367.
42. Schwertz FA, Brow JE. Diffusivity of water vapor in some common gases. *J Chem Phys*. 1951;19:640–646.
43. Winkelmann A. Über die diffusion von gasen und dämpfen. *Wied Ann*. 1884;22:152–161.
44. Xu B, Nagashima K, DeSimone JM, Johnson CS. Diffusion of water in liquid and supercritical carbon dioxide: an NMR study. *J Phys Chem A*. 2003;107:1–3.
45. Poling BE, Prausnitz JM, O'Connell JP. *The Properties of Gases and Liquids*, 5th ed. New York: McGraw-Hill, 2001.
46. Skelland AHP. *Diffusional Mass Transfer*. New York: Wiley, 1974.
47. Othmer DF, Thakar MS. Correlating diffusion coefficients in liquids. *Ind Eng Chem*. 1953;45:589–593.
48. Wilke CR, Chang P. Correlation of diffusion coefficients in dilute solutions. *AIChE J*. 1955;1:264–270.
49. Scheibel EG. Physical chemistry in chemical engineering design. *Ind Eng Chem*. 1954;46:1569–1579.
50. Hayduk W, Laudie H. Prediction of diffusion coefficients for nonelectrolytes in dilute aqueous solutions. *AIChE J*. 1974;20:611–615.
51. Tyn MT, Calus WF. Diffusion coefficients in dilute binary liquid mixtures. *J Chem Eng Data*. 1975;20:106–109.
52. Nakanishi K. Prediction of diffusion coefficient of noneletrolytes in dilute solution based on generalized Hammond-Stokes plot. *Ind Eng Chem Fundamen*. 1978;17:253–256.
53. Hayduk W, Minhas S. Correlations for prediction of molecular diffusivities in liquids. *Can J Chem Eng*. 1982;69:295–299.
54. Siddiqi MA, Lucas K. Correlation for prediction of diffusion in liquids. *Can J Chem Eng*. 1986;64:839–843.
55. Wilke CR, Lee CY. Estimation of diffusion coefficients for gases and vapors. *Ind Eng Chem*. 1955;47:1253–1257.
56. Fuller EN, Schettler PD, Giddings JC. A new method for prediction of binary gas-phase diffusion coefficients. *Ind Eng Chem*. 1966;58:19–27.
57. Brokaw RS. Predicting transport properties of dilute gases. *Ind Eng Chem Process Des Dev*. 1969;8:240–253.
58. Riazi MR, Whitson CH. Estimating diffusion coefficients of dense fluids. *Ind Eng Chem Res*. 1993;32:3081–3088.
59. Anslyn EV, Dougherty DA. *Modern Physical Organic Chemistry*. California: University Science Books, 2006.
60. Raveendran P, Ikushima Y, Wallen SL. Polar attributes of supercritical carbon dioxide. *Acc Chem Res*. 2005;38:478–485.
61. Buckingham AD, Disch RL. The quadrupole moment of the carbon dioxide molecule. *Proc R Soc London*. 1963;273:274–289.
62. Sato H, Matubayasi N, Nakahara M, Hirata F. Which carbon dioxide is more soluble? Ab initio study on carbon monoxide and dioxide in aqueous solution. *Chem Phys Lett*. 2000;323:257–262.
63. Linstrom PJ, Mallard WG. *NIST Chemistry WebBook*, NIST Standard Reference Database 69; 2005.
64. Gubskaya AV, Kusalik PG. The total molecular dipole moment for liquid water. *J Chem Phys*. 2002;117:5290–5302.
65. Gubskaya AV, Kusalik PG. The multipole polarizabilities and hyperpolarizabilities of the water molecule in liquid state: an ab initio study. *Mol Phys*. 2001;99:1107–1120.
66. Lide DR, editor. *CRC Handbook of Chemistry and Physics*, 90th ed. Boca Raton, FL: CRC Press, 2010.
67. Uematsu M, Frank EU. Dielectric constant of water and steam. *J Phys Chem Ref Data*. 1980;9:1291–1306.
68. Cussler EL. *Diffusion Mass Transfer in Fluid Systems*. UK: Cambridge University Press, 2009.
69. Hirschfelder JO, Curtiss CF, Bird RB. *Molecular Theory of Gases and Liquids*. USA: Wiley, 1954.
70. Gubbins KE, Bhatia KK, Walker RD. Diffusion of gases in electrolyte solutions. *AIChE J*. 1966;12:548–552.

71. Sahores KJ, Witherspoon PA. *Advances in Organic Geochemistry*. UK: Pergamon Press, 1970.
72. Lu WJ, Chou IM, Burruss RC, Yang MZ. In situ study of mass transfer in aqueous solutions under high pressures via Raman spectroscopy: a new method for the determination of diffusion coefficients of methane in water near hydrate formation conditions. *Appl Spectrosc*. 2006;60:122–129.
73. Witherspoon PA, Saraf DN. Diffusion of methane, ethane, propane, and *n*-butane in water from 25 to 43°C. *J Phys Chem*. 1965;69: 3752–3755.
74. Witherspoon PA, Bonoli L. Correlation of diffusion coefficients for paraffin, aromatic, and cycloparaffin hydrocarbons in water. *Ind Eng Chem Fundamen*. 1969;8:589–591.
75. Halmour N, Sandall OC. Molecular diffusivity of hydrogen sulfide in water. *J Chem Eng Data*. 1984;29:20–22.
76. Dhima A, de Hemptinne J, Jose J. Solubility of hydrocarbons and CO_2 mixtures in water under high pressure. *Ind Eng Chem Res*. 1999;38:3144–3161.
77. Leahy-Dios A, Firoozabadi A. Unified model for nonideal multicomponent molecular diffusion coefficients. *AIChE J*. 2007;53:2932–2939.
78. Bahadori A, Vuthaluru HB, Mokhatab S. New correlations predict aqueous solubility and density of carbon dioxide. *Int J Greenhouse Gas Control*. 2009;3:474–480.
79. Houghton G, McLean AM, Ritchie PD. Compressibility, fugacity, and water-solubility of carbon dioxide in the region 0–36 atm and 0–100°C. *Chem Eng Sci*. 1957;6:132–137.
80. Mather AE, Franck EU. Phase equilibria in the system carbon dioxide—water at elevated pressures. *J Phys Chem*. 1992;96:6–8.
81. Takenouchi S, Kennedy GC. The binary system H_2O-CO_2 at high temperatures and pressures. *Am J Sci*. 1964;262:1055–1074.
82. Lucia A. A mustiscale Gibbs-Helmholtz constrained cubic equation of state. *J Thermodynamics*. 2010;238365:1–10.
83. Fick A. On liquid diffusion. *J Sci*. 1855;10:30–39.
84. Vignes A. Diffusion in binary solutions. *Ind Eng Chem Fundamen*. 1966;5:189–199.
85. Caldwell CS, Babb AL. Diffusion in ideal binary liquid mixtures. *J Phys Chem*. 1956;60:51–60.

Appendix: Framework for Calculating Fickian Diffusion Coefficients in Binary Mixtures

In any mixture, diffusive flux is driven by concentration gradient (molecular diffusion), temperature gradient (thermal diffusion), and pressure gradient (pressure diffusion). In a binary mixture under isothermal and isobaric conditions, molecular diffusion—appropriately termed Fickian diffusion—can be expressed via Fick's law[7,83] as,

$$\vec{J}_1 = -cD\nabla x_1, \tag{A1}$$

where, $\vec{J}_1$ is the molar diffusive flux (mol/m^{2}s) of component 1, ∇x_1 is the gradient of mole fractions of component 1 (m^{-1}), c is mixture's molar density (mol/m^3), and D is the Fickian diffusion coefficient (m^2/s) for the mixture.

Alternatively, Fickian diffusion at constant temperature and pressure, can be written using the Stefan-Maxwell (SM) approach[7]:

$$\vec{J}_1 = -c\wp\Gamma\nabla x_1, \tag{A2}$$

where, $\wp$ is the SM diffusion coefficient, and Γ is the thermodynamic factor that represents the mixture's nonideality as a function of the fugacity[77] of component 1, f_1:

$$\Gamma = x_1 \frac{\partial \ln f_1}{\partial x_1}\bigg|_{T,P}. \tag{A3}$$

A general practice in literature is to use activity coefficients[7] to calculate nonideality; however, in our work, we use fugacity calculated from an appropriate EOS, since it more accurately predicts pressure effects on nonideality.

Comparison of Eqs. A1 and A2 provides the relation between SM and Fickian diffusion coefficients:

$$D = \wp\Gamma. \tag{A4}$$

Equality of $\wp$ and D is achieved at the infinite dilution limit (at $\Gamma = 1$), where the diffusion coefficient is denoted as D^∞. In concentrated mixtures, D is calculated from Eq. A4, where $\wp$ is estimated from the proposed D^∞ model (Eq. 1) by accounting for the mixture's composition. In general, either the geometric mean, proposed by Vignes[84] or the arithmetic mean suggested by Caldwell and Babb[85] are commonly used. In this work we use the Vignes mixing rule:

$$\wp = \left(D_{12}^\infty\right)^{x_2}\left(D_{21}^\infty\right)^{x_1}. \tag{A5}$$

Manuscript received Mar. 21, 2010, and revision received Jun. 22, 2010.